Biochimie 142 (2017) 22–30

Contents lists available at ScienceDirect

Biochimie

journal homepage: www.elsevier.com/locate/biochi

Research paper

Residue specific effects of human islet polypeptide amyloid on self-assembly and on cell toxicity

Lucie Khemtemourian [a, b, c, *], Ghislaine Guillemain [d, e, f], Fabienne Foufelle [d, e, f], J. Antoinette Killian [g]

[a] Sorbonne Universités, UPMC, Univ Paris 06, Laboratoire des Biomolécules, 4 place Jussieu, F-75005, Paris, France
[b] Ecole Normale Supérieure-PSL Research University, Département de Chimie, 24 rue Lhomond, F-75005, Paris, France
[c] CNRS, UMR 7203, Laboratoire des Biomolécules, F-75005, Paris, France
[d] INSERM, UMR_S 1138, Centre de Recherche des Cordeliers, F-75006, Paris, France
[e] Sorbonne Universités, UPMC, Univ Paris 06, UMR_S 1138, Centre de Recherche des Cordeliers, F-75006, Paris, France
[f] Université Paris Descartes, Sorbonne Paris Cité, UMR_S 1138, Centre de Recherche des Cordeliers, F-75006, Paris, France
[g] Department of Chemistry, Faculty of Science, Membrane Biochemistry and Biophysics, Bijvoet Center for Biomolecular Research, Padualaan 8, 3584, Utrecht, The Netherlands

ARTICLE INFO

Article history:
Received 17 March 2017
Accepted 29 July 2017
Available online 2 August 2017

Keywords:
Islet amyloid polypeptide
Amyloid
Amyloid-inhibitor
Type 2 diabetes mellitus
Aggregation

ABSTRACT

Type 2 diabetes mellitus is characterized histopathologically by the presence of fibrillary amyloid deposits in the pancreatic islets of Langerhans. Human islet amyloid polypeptide (hIAPP), the 37-residue pancreatic hormone, is the major constituent of these amyloid deposits. The propensity of IAPP to form amyloid fibrils is strongly dependent on its primary sequence. An intriguing example is His at residue 18. Although H18 is located outside the amyloidogenic region, it has been suggested that this residue and its charge state play an important role in the kinetics of conformational changes and fibril formation as well as in mediating cell toxicity. To gain more insight into the importance of this residue, we have synthesized four analogues (H18R-IAPP, H18K-IAPP, H18A-IAPP and H18E-IAPP) and we performed a full biophysical study on the properties of these peptides. Kinetic experiments as monitored by thioflavin-T fluorescence, transmission electron microscopy, circular dichroism and cell toxicity assays revealed that all variants are less fibrillogenic and less toxic than native hIAPP both at neutral pH and at low pH. This demonstrates that the effect of H18 in native IAPP is not simply determined by its charge state, but rather that residue 18 is important for specific intra- and intermolecular interactions that occur during fibril formation and that may involve charge, size and hydrophobicity. Furthermore, our results indicate that H18R-IAPP has a strong inhibiting effect on native hIAPP fibril formation. Together these results highlight the large impact of modifying a single residue outside the amyloidogenic domain on fibril formation and cell toxicity induced by IAPP, opening up new avenues for design of inhibitors or modulators of IAPP aggregation.

1. Introduction

Amyloid is a fibrous quaternary structure formed by the aggregation of monomeric protein or peptide into a cross β-sheet fold. A wide range of pathologies, including Alzheimer's disease, Parkinson's disease, Huntington disease and type 2 diabetes mellitus (T2DM), is associated with the formation of amyloid fibrils [1]. For each of these diseases, a specific protein is involved in the amyloid assembly, leading to cell degeneration and cell death.

In T2DM the main constituent of islet amyloid is the islet amyloid polypeptide, IAPP, which displays amino acid sequence homology with calcitonin gene-related peptides [2,3]. IAPP is a 37-residue polypeptide pancreatic hormone coproduced and consecrated with insulin in a molar ratio of about 1:100 in healthy

Abbreviations: IAPP, Islet Amyloid Polypeptide; CD, circular dichroism; T2DM, type 2 diabetes mellitus; TEM, transmission electron microscopy; ThT, Thioflavin T.

* Corresponding author. CNRS, UMR 7203, Laboratoire des Biomolécules, F-75005, Paris, France.
E-mail address: lucie.khemtemourian@upmc.fr (L. Khemtemourian).

http://dx.doi.org/10.1016/j.biochi.2017.07.015
0300-9084/

individuals, but in a ratio of about 1:20 in T2DM [4,5]. The formation and the deposition of IAPP amyloid in the islets of Langerhans of the pancreas is a typical pathological feature of T2DM. A strong correlation was shown between the occurrence of T2DM in a particular species and the primary sequence and amyloid forming propensity of the IAPP that is produced by that species. For example, rat or mouse IAPP (rIAPP or mIAPP) differs from human IAPP by six residues out of 37, does not form fibrils and rats or mice do not spontaneously develop T2DM, whereas cat IAPP differs from human IAPP by four residues, does form amyloid fibrils and cats do develop the disease [6,7]. Therefore, understanding particular sequence/structure relationships is likely to be essential in defining why some amyloids do form toxic amyloids and others do not.

In general, the ability of a peptide to form amyloid fibrils is dependent on i) the presence of hydrophobic amino-acids with a high β-sheet propensity, ii) the presence of aromatic residue especially phenylalanine and tryptophan, iii) the lack of prolines and iv) the presence of electrostatic interactions [8–12]. To investigate possible amyloidogenic regions in full length human IAPP (hIAPP), several research groups have synthesized truncated and mutated peptides and studied their amyloidogenic properties using biophysical and biological techniques [13–15]. It was shown that the mutations within the 20–29 region induce an important alteration on IAPP amyloid formation. Nevertheless, this segment is not the sole domain determining its amyloidogenic propensity. Multiple proline substitutions outside this region could also induce a loss in IAPP amyloid formation, as for example, mutations within the N14, F15, L16, V17 residues [8,14,15]. Previous studies suggest that residue 18 may have a critical role in mediating cell toxicity [16,17]. In addition, studies at different pH indicated that the ionization state of histidine 18 significantly affects the kinetics of conformational changes and concomitant fibril formation [18]. Importantly, one difference between the sequence of hIAPP and non-amyloidogenic mIAPP is the substitution of histidine 18 of hIAPP with an arginine in mIAPP. Green and co-workers have synthesized a mutated mIAPP where arginine 18 has been replaced by histidine 18, and reported that this modified mIAPP was able to form fibrils, underlining the importance of residue 18 and the potential role of its charge state for hIAPP structure and fibril formation [19].

To gain more insight into the importance of residue 18 for the intermolecular IAPP interactions that are essential for fibril formation, we here have synthesized four mutated peptides where histidine 18 has been replaced by arginine (H18R-IAPP), lysine (H18K-IAPP), glutamic acid (H18E-IAPP) and alanine (H18A-IAPP) to achieve variations in charge, size and polarity. We report a full biophysical study of the behavior of these mutated peptides in comparison with that of native hIAPP. We determined the ability of the mutated peptides to form fibrils, their secondary structure and their toxicity towards INS-1 β-cells. Finally, the properties of the peptides at pH 5.5 and pH 7.4 were compared to allow comparison with effects of pH on native hIAPP [18]. It also should be noted that both pH values are physiologically relevant: mature hIAPP is stored in the β-cell granules of the pancreas at a pH of approximatively 5.5 and released into the extracellular compartment, which has a pH of 7.4. Our results show that all mutated peptides are less prone to aggregation and less toxic to INS-1 β-cells than wild-type hIAPP, even though the mutation is outside the amyloidogenic domain. This was observed for both values of pH, indicating that the previously observed pH dependent differences in aggregation of hIAPP [18] are not solely due to differences in the charge state of H18. Rather, the results suggest that residue 18 is involved in specific intra- and intermolecular interactions that are important for fibril formation and that involve charge, size and hydrophobicity.

2. Materials and methods

2.1. Peptide synthesis

All peptides were synthesized with a CEM Liberty Blue (CEM corporation, Matthews, USA) automated microwave peptide synthesizer using standard reaction cycles at the Institut de Biologie Intégrative (IFR83-Université Pierre et Marie Curie) as described [20]. The synthesis of all IAPP with an amidated C-terminus and a disulfide bridge were performed using Fmoc chemistry and a PAL Novasyn TG resin. Two pseudoproline dipeptides were chosen for the synthesis Fmoc-Ala-Thr(ΨMe,MePro)-OH replaced residues Ala-8 and Thr-9, and Fmoc-Leu-Ser(ΨMe,MePro)-OH replaced residues Leu-27 and Ser-28. Double couplings were performed for the pseudoprolines and for the residues following the pseudoprolines and for every β-branched residue. The peptides were cleaved from the resin and deprotected using standard TFA procedures with 1,2-ethanedithiol, water, and triisopropylsilane as scavengers. The peptides were purified by reverse phase high-performance liquid chromatography (HPLC) with a Luna C18(2) column (Phenomenex, USA). A two-buffer system was used. Buffer A consisted of 100% H2O and 0.1% TFA (vol/vol), and buffer B consisted of 100% acetonitrile and 0.07% TFA (vol/vol). Linear peptides were dissolved in aqueous DMSO (33%) and oxidized with air to the corresponding disulfide bond. Purity of peptides was higher than 95% as determined by analytical HPLC and identity of peptides was confirmed by MALDI-TOF mass spectrometry.

2.2. Sample preparation

An essential criterion for measuring aggregation kinetics of amyloid peptides is to start with a monomeric form of the peptide. Therefore, peptide stock solutions were freshly prepared prior to all experiments using the same batch. Peptide stock solutions were prepared as described previously [21]. Briefly, stock solutions obtained by dissolving the peptide at a concentration of 1 mM in hexafluoroisopropanol (HFIP) and by leaving it to incubate for an hour. Then, HFIP was evaporated and the sample was dried by vacuum desiccation for at least 30 min. The resulting peptide film was dissolved at a concentration of 1 mM in DMSO for the fluorescence experiments (final DMSO concentration of 2.5% v/v) and then diluted in 10 mM sodium phosphate buffer, 100 mM NaCl (pH 7.4 or pH 5.5). Both DMSO and NaCl interfere with the circular dichroism experiments, and therefore in these experiments the peptide film was directly dissolved in a 10 mM sodium phosphate buffer, 100 mM NaF (pH 7.4 or pH 5.5). It is important to note that NaF may slow down the β-sheet transition as compared to NaCl [22]. For the cytotoxicity assay the peptide film was directly dissolved in the culture media.

2.3. Circular dichroism

The secondary structure of peptides was measured using a Jasco J-815 CD spectropolarimeter with a Peltier temperature-controlled cell holder over the wavelength range 190–260 nm. Measurements were carried out in cells of 0.1 cm path length at 25 °C in 10 mM phosphate buffer, 100 mM NaF (pH 7.4 or pH 5.5). Measurements were taken every 0.2 nm at a scan rate of 20 nm/min. Each spectrum reported is the average of four scans. Peptide concentration was 25 μM. The background spectrum was subtracted and the results were expressed as mean residue molar ellipticity [θ].

2.4. Fluorescence assays

The kinetics of fibril formation was measured using the fluorescence intensity increase upon binding of the fluorescent probes Thioflavin T (ThT) to fibrils. A plate reader (Fluostar Optima, BMG LabTech, Germany) and a standard 96 wells black microtiter plate were used. Prior the first measurement, the plate was shaken at 600 rpm for 10 s. The fluorescence was measured at room temperature from the top of the plate every 10 min with excitation filter 440 nm and emission filter 480 nm.

The fluorescence assay was started by adding 10 μL of a 0.2 mM IAPP in DMSO to 190 μL of a mixture of 10 μM ThT and 10 mM phosphate buffer, 100 mM NaCl (pH 7.4 or pH 5.5). For the hIAPP:H18R-IAPP experiments, the ThT assay was started by adding 10 μL of a 0.2 mM h-IAPP and 10 μL of a 0.2 mM H18R-IAPP to 180 μL of a mixture of 10 μM ThT and 10 mM phosphate buffer, 100 mM NaCl (pH 7.4 or pH 5.5). The assays were performed 3 times, each in triplicate, on different days, using different hIAPP stock solutions. The replicates of each system showed consistent reproducibility.

The resulting curves can be processed by a sigmoidal Boltzmann equation. This fitting allows the estimation of kinetic parameters such as the time for which the fluorescence reaches 50% of its maximal intensity ($t_{1/2}$).

$$F = \frac{Fi - Ff}{1 + e^{(t - t1/2)/\tau}} + Ff$$

2.5. Electron microscopy

TEM was performed at the “Institut de Biologie Paris Seine” (IBPS, Paris, France) at the University Pierre and Marie Curie. Aliquots (20 μL) of the samples used for fluorescence assays were removed at the end of each kinetic experiments, blotted on a glow-discharged carbon coated 200 mesh copper grids for 2 min and then negatively stained with saturated uranyl acetate for 45 s. Grids were examined using a ZEISS 912 Omega electron microscope operating at 80 kV.

2.6. Cell culture

Rat insulinoma-1 (INS-1) pancreatic β-cells were grown in culture medium containing RPMI 1640 supplemented with penicillin (100 units/ml), streptomycin (100 μg/ml), β -mercapto-ethanol (50 μM), pyruvate (1 μM) and 10% heat-inactivated calf serum. The cultures were maintained at 37 °C in humidified 95% air, 5% CO_2.

2.7. MTT cell toxicity assay

MTT-based cell toxicity assay was used to assess cell metabolic activity [23]. The cell growth is measured as a function of mitochondrial activity in living cells. Low absorbance values indicate a reduction in cell viability. The MTT cell assays were performed according to the manufacturer's instructions (Sigma Aldrich, France). Briefly, the INS-1 cells were plated at a density of 30 000 cells/well in a 96-wells plate. Following 24 h of incubation, the medium was replaced with 100 μL of fresh medium containing 50 μM of indicated peptide. Cells were further incubated for 24 h 10 μL of MTT solution (5 mg/mL) was added to each well and further incubated for 3 h. After this incubation period, the culture medium was removed and 100 μL of MTT solvent were added. The well-plate was gently shaken during 30 min and the absorbance was measured at 550 nm within 1 h after adding MTT solvent. Values were calculated relative to those of control cells treated with buffer only. The assays were performed 4 times, each in triplicate, on different cell line cultures, using different hIAPP stock solutions. All values represent means ± the standard error of the mean (N = 4).

3. Results

3.1. Design of mutated peptides

Recent work has demonstrated that the rate of fibril formation and the random coil to β-sheet transition are slower at pH 5.5 than at pH 7.4 [18]. Since residue histidine 18 is the only residue that titrates over this pH range, it was suggested that it is the ionization state of the histidine that affects the kinetics of fibril formation and of the conformational changes. These observations suggest that mutation of the residue 18 and changing its charge may significantly modulate the rate of IAPP fibril formation and IAPP toxicity. Thus, we synthesized four mutated peptides, where histidine 18 was replaced by arginine, lysine, glutamic acid, and alanine (Fig. 1). The Arg and Lys substitutions were chosen because both are positively charged amino acids and have a roughly similar volume [24,25]. However, Arg is less hydrophobic than Lys which is also less hydrophobic than His. The Glu substitution permits to have a negatively charged amino acid with approximately a similar volume and hydrophobicity as His, while the uncharged Ala is more hydrophobic and has a smaller volume.

3.2. Mutated peptides adopt a stable random coil conformation

CD spectroscopy was used to investigate the secondary structure of peptides at the start of incubation (Fig. 2A) and after 24 h of incubation (Fig. 2B). The CD spectra of peptides freshly dissolved in 50 mM phosphate buffer, 100 mM NaF at 25 μM are nearly identical, displaying a peak with negatively ellipticity at 200 nm that is characteristic of a random coil conformation. After 24 h of incubation, hIAPP adopts a β-sheet structure, indicated by the appearance of a negative band at 220 nm and the loss of the negative band at 200 nm. In contrast, the CD signals of the mutated peptides show that these peptides retain their random coil conformation for at least 24 h, indicative of the absence of amyloid fibril formation under these conditions. This result suggests that the mutated

hIAPP	K C N T A T C A T Q R L A N F L V **H** S S N N F G A I L S S T N V G S N T Y
H18K	K C N T A T C A T Q R L A N F L V **K** S S N N F G A I L S S T N V G S N T Y
H18R	K C N T A T C A T Q R L A N F L V **R** S S N N F G A I L S S T N V G S N T Y
H18E	K C N T A T C A T Q R L A N F L V **E** S S N N F G A I L S S T N V G S N T Y
H18A	K C N T A T C A T Q R L A N F L V **A** S S N N F G A I L S S T N V G S N T Y
mIAPP:	K C N T A T C A T Q R L A N F L V **R** S S N N **L** G **P V** L **P P** T N V G S N T Y

Fig. 1. Primary sequence of native human IAPP (blue), the mutated peptides (H18K, red; H18R, purple; H18E, green; and H18A, yellow) and mIAPP (dark blue). Each peptide contains a disulfide bond (Cys2 and Cys7) and an amidated C-terminus.

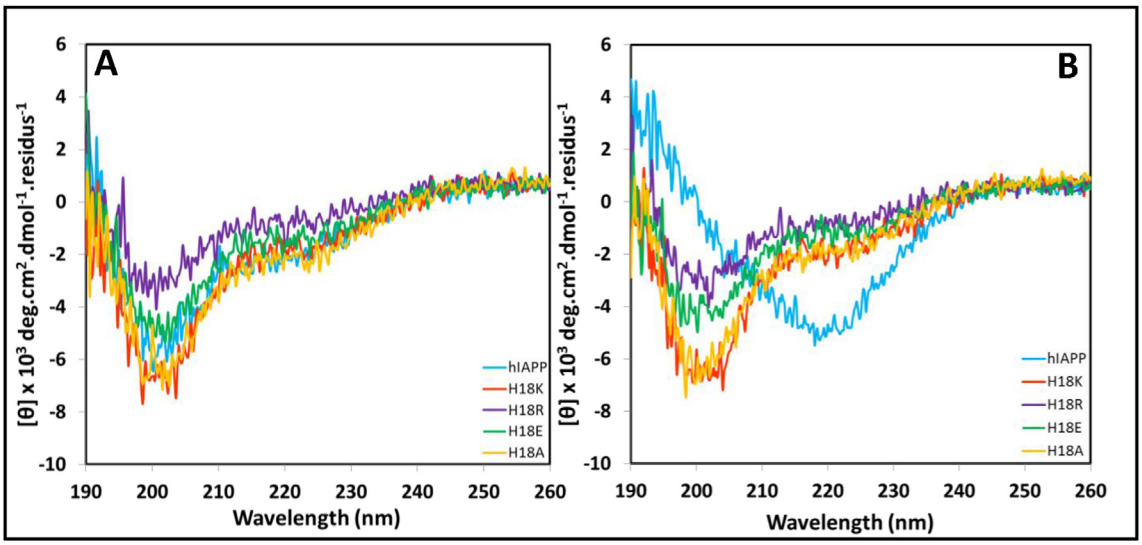

Fig. 2. CD spectra of 25 μM native hIAPP (blue) and the mutative peptides (H18K, red; H18R, purple; H18E, green; and H18A, yellow) freshly dissolved in 50 mM phosphate buffer, 100 mM NaF (A) and after 24 h of incubation (B) at pH 7.4.

peptides have no or a lower amyloidogenic potential than hIAPP.

3.3. Mutated peptides are less amyloidogenic than hIAPP

Next, we tested the propensity of the different mutated peptides to form amyloid at pH 7.4 using thioflavin-T (ThT) fluorescence assays and transmission electron microscopy (TEM). ThT is a small dye and one of the most commonly used for amyloid detection [26]. The aggregation of amyloid peptides can be described by a sigmoidal transition with a well-defined lag phase in which monomers and oligomers dominate the population, followed by a growth phase during which fibrils elongate and, finally, a plateau [27]. The kinetics data can be fitted according to a Boltzmann sigmoidal equation. Two parameters can be derived from the ThT curves: the time at half fibril conversion ($t_{1/2}$) and the fluorescence intensity at the plateau. Fig. 3A show typical sigmoidal curves obtained for native hIAPP and the mutated peptides. For hIAPP, the transition from monomer to fibril formation occurs at 2.8 ± 0.2 h and the saturation phase is reached within 5 h. Clear differences in the kinetics profile of hIAPP and the mutated peptides are observed in terms of initial lag-time and the equilibrium plateau. Our data show an increase in the $t_{1/2}$ depending on the peptide: for H18K-IAPP around 10 h (compared to 2.8 h for native hIAPP), for H18E-IAPP 20 h, for H18R-IAPP 33 h and for H18A-IAPP 35 h. This clearly indicates that the mutated peptides have a lower amyloidogenic property following the order of fibrillogenicity: 18H > 18K > 18E > 18R, 18A. In addition, except for H18E-IAPP, all the mutated peptides have a reduced final fluorescence intensity, by a factor 1.6 for H18K-IAPP and 5.5 for H18R-IAPP and H18A-IAPP. The ThT signal derives from the complex fibril-dye and the intensity of the plateau is highly dependent on the binding between the fibrils and the dye. Thus, it is critical to assay fibril formation by another method, such as TEM. We conducted TEM of the samples collected after 3 days of incubation. hIAPP fibrils exhibit the typical morphology of amyloid fibrils with diameters between 10 and 15 nm (Fig. 3B). Similar observations are made for both H18K-IAPP and H18E-IAPP (Fig. 3C, E). However, the morphology of the fibrils of H18R-IAPP and H18A-IAPP is somewhat different. We observe mainly relatively short fibrils that do not appear to have strong propensity to cluster into a more dense regular pattern (Fig. 3D, F).

3.4. The mutated peptides are less toxic to β-cells

To investigate the relationship between conformational changes of peptides, fibril formation and cell toxicity, we tested the mutated peptide on cell viability using rat INS-1 cells, a pancreatic cell line commonly used in studies of hIAPP toxicity. Cell viability was monitored by MTT assays for peptide samples at 50 μM. The non-fibrillogenic and nontoxic mouse IAPP peptide was used as a negative control. Consistent with previous reports, hIAPP exhibits strong cytotoxicity at a concentration of 50 μM, as quantified in Fig. 4, with cell viability being reduced to 16 ± 8% relative to the control cells after 24 h of incubation. In contrast, in the presence of the mutated peptides at the same concentration, cell viability varies from ~54 to 63% and thus is strongly increased as compared to the effect of the wild-type. Control studies showed that mIAPP does not affect cell viability. These results suggest that the fibrillogenicity of the peptides is correlated to the toxicity.

3.5. H18R-IAPP inhibits fibril formation and cell toxicity of native hIAPP

Wild type IAPP contains a histidine residue at position 18, while mIAPP, which is nonamyloidogenic and not cytotoxic, contains an arginine at this position, as well as some other mutations in the amyloidogenic region. For mIAPP it was shown that it inhibits hIAPP fibril formation [28]. Thus, here we wanted to know whether H18R-IAPP might be able to interfere with hIAPP fibrillogenesis and toxicity. Our data show that addition of an equimolar amount of H18R-IAPP to hIAPP results in i) a reduction in the level of fibril formation from ~95% to ~50% (Fig. 5A), ii) an increase of the $t_{1/2}$ from ~2 h to ~9 h (Fig. 5B) and iii) an increase in cell viability from ~16% to ~35%. These results demonstrate that the H18R substitution, even though it is outside the amyloidogenic sequence, is able to cause a dramatic inhibition of both fibril formation and toxicity when this mutant peptide is added to wild-type IAPP.

3.6. Low pH inhibits fibril formation for the mutated peptides except for 18A-IAPP

It was previously shown that the rate of hIAPP fibril formation is faster at pH 7.4 than at pH 5.5 [18]. Thus, we next investigated the

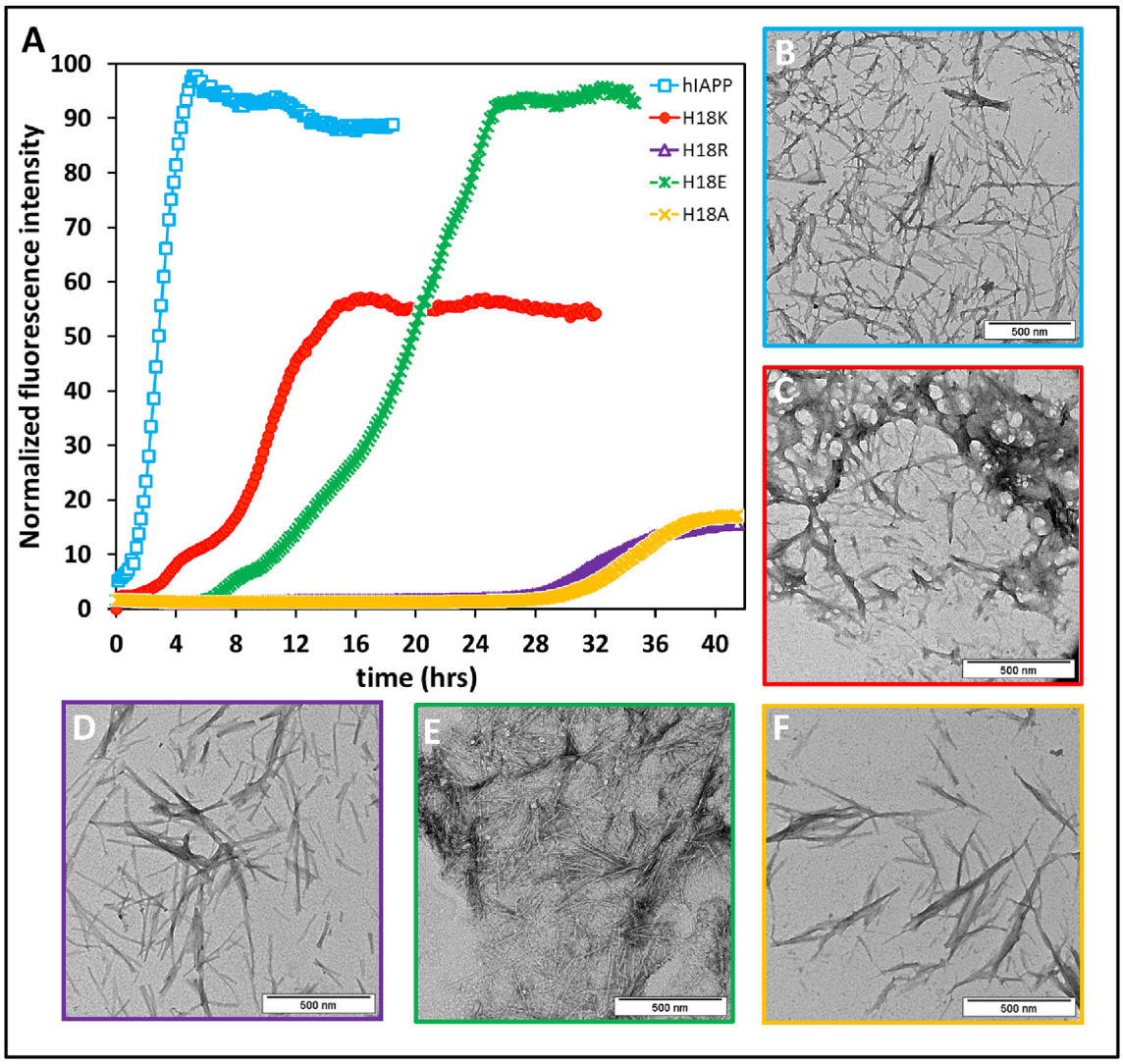

Fig. 3. (A) Kinetics of native hIAPP and the mutated IAPP (H18K, red; H18R, purple; H18E, green; and H18A, yellow) fibril formation at 10 μM in 50 mM phosphate buffer, 100 mM NaCl at pH 7.4. (B to F) Negatively stained microscopy images of native hIAPP (B) and mutated IAPP (H18K, C; H18R, D; H18E, E; and H18A, F).

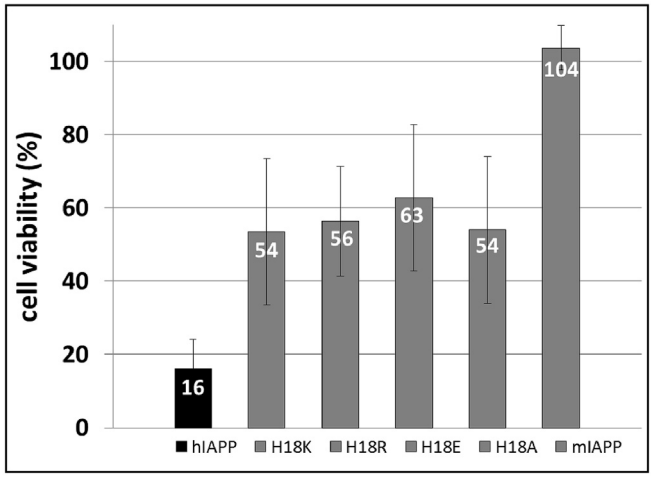

Fig. 4. Comparison of cell toxicity induced by native and mutated IAPP at a peptide concentration of 50 μM. Cell viability was measured after incubation of INS-1 β-cells with the peptides for 24 h. Cell viability was assessed using MTT assays. Errors bars represent the standard deviation determined from four repeated measurements.

effect of an acidic pH on the mutated peptides. First, we determined the secondary structure of the mutated peptides at pH 5.5 using CD spectroscopy (Fig. 6A). The CD spectrum of mutated and wild type peptides freshly dissolved in 50 mM phosphate buffer, 100 mM NaF at 25 μM displays a peak with negative ellipticity at 200 nm that is characteristic of a random coil conformation. After 24 h of incubation the mutated peptides and hIAPP retain their random coil conformation, suggesting that a low pH inhibits fibril formation in agreement with a previous report [18]. This result is confirmed with TEM showing at pH 5.5 thinner and smaller fibrils with a lower frequency compared to the fibrils formed at pH 7.4 for wild type IAPP and H18K-, H18R- and H18E-IAPP (Fig. 6B–E). However, for H18A-IAPP, we observed a denser network with thicker fibrils at pH 5.5 than at pH 7.4 (Fig. 6F). Next, ThT experiments were carried out at pH 5.5 and the results were compared to those at pH 7.4. The $t_{1/2}$ time required to reach half-value of the maximum of the fluorescence intensity is reported in Fig. 6G for pH 7.4 (plain bars) and pH 5.5 (dash bars). Our data indicate that $t_{1/2}$ is higher for all the peptides at pH 5.5 than at pH 7.4, except for H18A-IAPP. These results are consistent with the TEM data, which also suggest that the kinetics of fibril formation is slower at pH 5.5 than at pH 7.4 for all peptides except for H18A-IAPP.

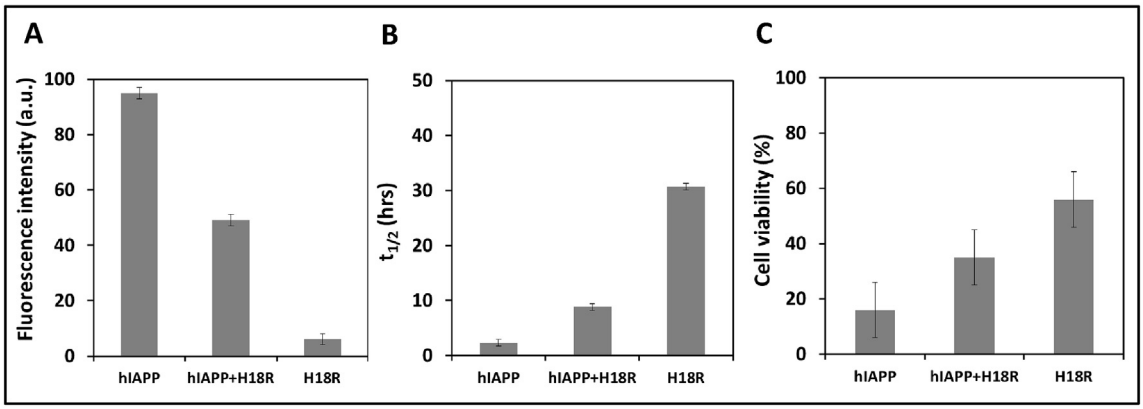

Fig. 5. Inhibition of native hIAPP fibril formation and cell toxicity by the mutated H18R-IAPP after incubation of 24 h. (A) Fluorescence intensity of the plateau region and (B) average midpoints ($t_{0.5}$) of the sigmoidal transition are shown for native hIAPP (10 μM), for mutated H18R-IAPP (10 μM) and for an equimolar mixture of hIAPP and H18R-IAPP (both at 10 μM) as determined by ThT fluorescence. (C) hIAPP cell toxicity for native hIAPP (50 μM), for mutated H18R-IAPP (50 μM), and for an equimolar mixture of hIAPP and H18R-IAPP (both at 50 μM), assessed by MTT assays.

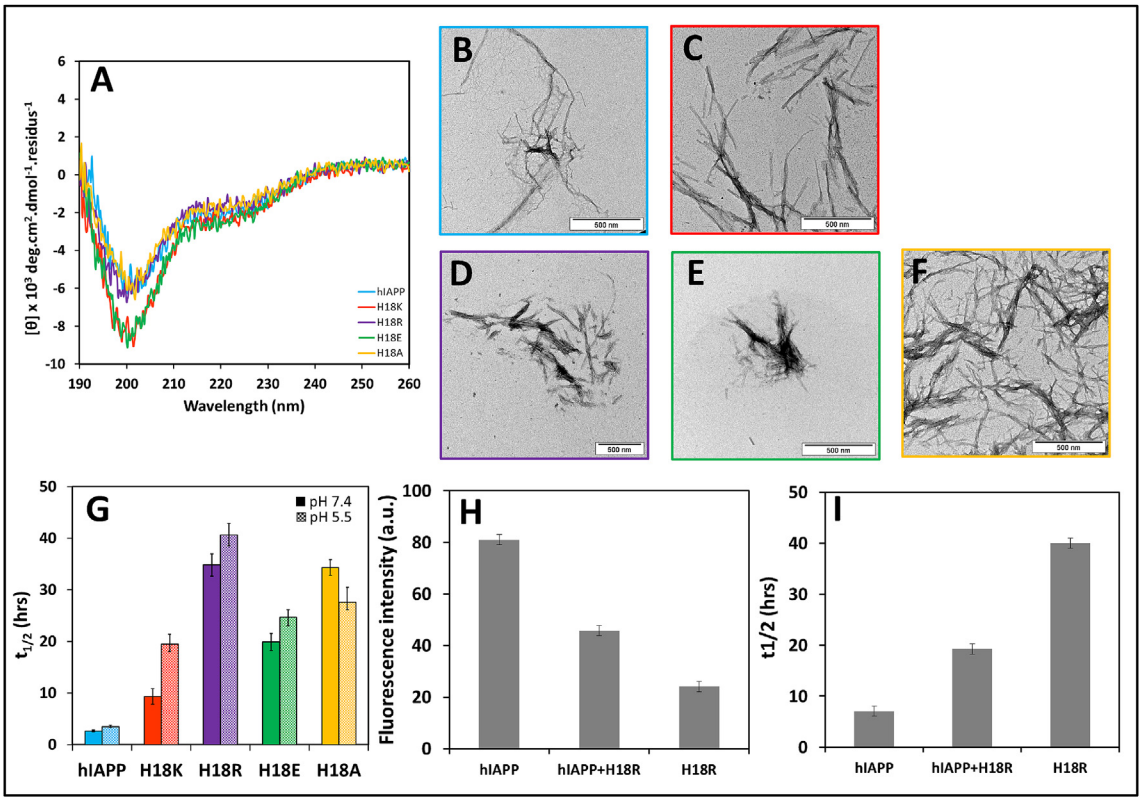

Fig. 6. CD spectra of 25 μM native hIAPP (blue) and the mutated peptides (H18K, red; H18R, purple; H18E, green; and H18A, yellow) freshly dissolved in 50 mM phosphate buffer, 100 mM NaF at pH 5.5 (A). Native hIAPP (B) and mutated IAPP (H18K, C; H18R, D; H18E, E; and H18A, F) in 50 mM phosphate buffer, 100 mM NaCl at pH 5.5. (G) Calculated half-times ($t_{0.5}$) of native IAPP and mutated IAPP (H18K, red; H18R, purple; H18E, green; and H18A, yellow) determined by ThT-fluorescence at pH 7.4 (plain bars) and pH 5.5 (dashed bars). Inhibition of native hIAPP fibril formation by the mutated H18R-IAPP determined by ThT fluorescence after incubation of 24 h, at pH 5.5. The average midpoints ($t_{0.5}$) of the sigmoidal transition (H) and the fluorescence plateau (I) are shown for native IAPP (10 μM), mutated H18R-IAPP (10 μM) and for the mixture hIAPP:H18R-IAPP (10 μM; 1:1 M ratio).

Finally, the influence of pH on the inhibition of hIAPP fibril formation by H18R-IAPP was investigated by ThT fluorescence. The experiment was performed with an equimolar amount of hIAPP and H18R-IAPP at a concentration of 5 μM. Our data show that also at a lower pH H18R-IAPP efficiently inhibits hIAPP fibril formation, the $t_{1/2}$ being reduced by a factor of 2.7 at pH 5.5. The addition of H18R-IAPP induced a reduction in the maximum of intensity from 81% to 46% (Fig. 6H) and an increase of the $t_{1/2}$ from 7.1 h to 19.3 h (Fig. 6I). These results demonstrate that i) a low pH inhibits fibril formation for the wild-type hIAPP and for the mutated peptides except H18A-IAPP and ii) H18R-IAPP is able to reduce the rate of native hIAPP fibril formation at a low pH as well as a physiological pH.

4. Discussion

hIAPP has been known to be the main component of the amyloid deposits that form in the pancreas of patients of T2DM. Despite

considerable progress, the mechanisms of amyloid fibril formation *in vitro* and *in vivo* are still not understood. Previously, it was shown that hIAPP fibril formation is strongly pH-dependent and it was postulated that this effect is directly related to the conformational behavior of hIAPP [18] and its cell cytotoxicity toward MIN6 mouse model pancreatic β-cells [29]. Since histidine at position 18 is the only residue of which the side chain titrates over the relevant pH range, both studies proposed that the ionization state of the histidine acts as an electrostatic switch that facilitates hIAPP fibril formation at physiological pH where histidine is uncharged and reduces the fibril formation at an acidic pH where histidine is charged. The data presented here reveal that this residue 18 contributes in a different and more complex way to IAPP amyloid assembly kinetics and toxicity, and that a single substitution, even with full retention of charge, has a profound effect on IAPP fibril formation and toxicity, as will be discussed now in more detail.

We have synthesized four mutated peptides where histidine 18 has been replaced by arginine, lysine, glutamic acid and alanine. To predict the amyloidogenicity of the five peptides, theoretical calculations were made using different algorithms. According to ZIPPER-DB, the amyloid propensity of hIAPP is decreasing when position 18 is a lysine, arginine and glutamic acid but increasing with an alanine [30]. Pawar et al. described a method for calculating the intrinsic amyloid aggregation propensities of a peptide and found the following order of amyloid propensities: A > H > K > E > R [31]. Finally, according to Sanchez de Groot, the experimental aggregation propensities of the amino acids follow the order: A > K > H > R > E [32]. Our experiments clearly show that all the mutated peptides, even H18A-IAPP, are less fibrillogenic than wild type hIAPP. The CD data show predominantly random coil structure for 24 h for all the analogues while the transition from random coil to β-sheet for hIAPP occurs after 4 h. This is consistent with the fluorescence and TEM data that show that the time course of ThT fluorescence and the quantity of fibrils observed by TEM are strongly dependent on residue 18 with the following order of fibrillogenicity: native hIAPP > H18K-IAPP > H18E-IAPP > H18R-IAPP, H18A-IAPP. It is important to note that the timescales in the CD measurements cannot be directly compared with those in the ThT experiments, since some agitation occurs during the fluorescence measurements, which has been shown to accelerate the kinetics of fibril formation [33]. Altogether, our results demonstrate that the effects of the substitutions are consistent. The cell toxicity experiments on INS 1 cells reveal that all the mutated peptides induce less toxicity than the wild type suggesting that His-18 is a requirement for high cell toxicity. Also here the strongest effects of the substitutions are observed for H18R-IAPP and H18A-IAPP. The conformational and aggregational features of the analogues were also explored at an acidic environment of 5.5, mimicking the pH of the secretory granules. The results show that the rate of fibril formation is slower at pH 5.5 compared to pH 7.4 for all the analogues except H18A-IAPP, showing that also hIAPP analogues with non-titratable amino acid side chains at position are sensitive to pH. This result is in line with results from recent study on an H18Q-hIAPP analogue [34]. Since arginine, lysine and the glutamic acid are permanently charged residues at pH 7.4 and pH 5.5, the charge cannot be the sole factor determining the properties of IAPP. We therefore suggest that the amyloidogenicity of a peptide is controlled by a combination of charged, hydrophobic and aromatic residues.

During the last decade, different analogues were designed, synthesized and their amyloidogenic properties were determined using biophysical techniques. hIAPP and non amyloidogenic mIAPP differ at six positions out of 37, namely positions 18, 23, 25, 26, 28 and 29 (Fig. 1), suggesting that the region 20–29 determines the ability of hIAPP to form fibrils. The first studies using proline substitutions within this 20-29 region demonstrated that this part is indeed essential in the process of fibril formation. Later, a number of mutations within residue 20 (Ser/Gly, Ser/Lys) were investigated and the results highlighted the importance of this residue in hIAPP structure and fibril formation [35–37]. In addition, multiple substitutions outside of the 20–29 region also led to non-amyloidogenic or less amyloidogenic peptides suggesting the importance of others regions such as 8–16, 13–19 and 31–37 [8,15,38,39]. Our study, revealing that histidine18 is important on allowing fibrillation to proceed, is consistent with a previous study that demonstrates that the mutation R18H is sufficient to render mIAPP amyloidogenic [19]. A more recent study has investigated the role of the C-terminal of IAPP and its interaction with the histidine 18 during IAPP amyloid formation [40]. In this study, residue histidine was replaced by leucine or glutamine. These two residues were chosen because they have approximately the same volume, however, leucine and glutamine are uncharged amino acids. In addition, glutamine and histidine have the same hydrophobicity index [25], while leucine is more hydrophobic. With the mutation H18L, hIAPP fibril formation was strongly accelerated while the fibril formation was moderately accelerated with the H18Q mutation, indicating that these mutation effects cannot be due only to the deletion of a positive charge [40].

Atomistic structural models of native hIAPP were calculated using data from scanning transmission electron microscopy, solid-state NMR and EPR as constraints [41,42]. The resulting family of structures exhibits fibril protofilaments that contain layers of β-sheets that twist around each other. The first model describes two β-strand segments, comprised of residues 8–17 and 28-37 separated by a bend or a loop, while the second model proposes two β-strand segments, comprised of residues 14–19 and 31–36. In both cases, residue 18 is at the interface between the β-sheet and the β-turn. The amino acids present in the β-sheet contribute to the constitution of the backbone of the fibrils while the amino acids present in the β-turn provide torsional flexibility for the β-sheet to form. The mutation of residue 18 at the interface between the β-sheet and the β-turn may destabilize the fibrils by decreasing the number of potential intra- and intermolecular hydrogen bonds as for example in the case of H18A-IAPP, or by changing the nature and/or the distance of the hydrogen bonds as in the case of H18R-IAPP and H18E-IAPP.

His18 is not only important for fibril formation and structure but also for binding of metal ions. In previous work, it was demonstrated that metal ions such as Cu(II), Ni(II) and Zn(II) prevent hIAPP fibril formation by anchoring to histidine 18 thereby inducing a change in the local conformation nearby the residue [43–45]. Similar experiments were done with Aβ, the amyloid peptide involved in Alzheimer's disease where it was concluded that modification of the three histidine residues (at positions 6, 13, and 14) of the peptide results in modulation of the aggregation and toxicity properties and affects the zinc binding [46–49].

Finally, another interesting observation in our study is that addition of 18R-IAPP modulates the properties of hIAPP. Indeed, the data presented here demonstrate that at a ratio 1:1, H18R-IAPP inhibits hIAPP-amyloid formation by lengthening the lag phase, reducing the final ThT fluorescence intensity and reducing the cytotoxicity towards INS-1 cells. A possible hypothesis is that the peptide-peptide interactions alter intra- or intermolecular hydrogen bonding and thereby slow down hIAPP fibril formation. It is interesting to note that the non-amyloidogenic mIAPP is a moderate inhibitor of native IAPP [28] while the single mutation H18R in native IAPP has a more pronounced inhibition effect on native IAPP. Indeed, previous results showed that adding mIAPP to hIAPP in a 1:1 M ratio increases $t_{1/2}$ by a factor of 2.5 [28], while our data reveal that addition of H18R-IAPP to hIAPP increases $t_{1/2}$ by a

factor of 4.5, suggesting a much stronger inhibiting effect. H18R-IAPP is as effective at inhibiting amyloid formation as a number of small molecules and peptide-based inhibitors [50,51] but less effective than others analogues of hIAPP where the mutations are located in the amyloidogenic region, as for example the I26P variant [52] or the double N-methylated hIAPP analogues [53,54].

It is known that changes in chemical composition in hIAPP can have dramatic effects on fibril assembly, structure and toxicity. Understanding precisely how the sequence influences structure may help to understand structure/function relationships in these amyloid forming proteins. The present works reveals the essential role of histidine in amyloid fibril formation and the impressive effect of a single mutation that is located outside the amyloidogenic region. We propose that this residue has such a strong effect because it is located at a crucial position in the assembled fibrils where small changes in precise chemical structure, charge properties and hydrogen-bonding interactions directly affect both intermolecular and intramolecular interactions between monomer units.

Author contributions

The research was performed in the university Pierre and Marie Curie (Paris, France) and in the research center “les cordeliers” (Paris, France). The manuscript was written through contributions of all authors. All authors have given approval to the final version of the manuscript.

Acknowledgements

Christophe Piesse (Institut de Biologie Paris Seine, Université Pierre et Marie Curie, France) is acknowledged for the peptides synthesis. We thank Michael Trichet (Institut de Biologie Paris Seine, Université Pierre et Marie Curie, France) for valuable discussions on electron microscopy.

References

[1] F. Chiti, C.M. Dobson, Protein misfolding, functional amyloid, and human disease, Ann. Rev. Biochem. 75 (2006) 333–366.
[2] G.J.S. Cooper, A.C. Willis, A. Clark, R.C. Turner, R.B. Sim, K.B.M. Reid, Purification and characterization of a peptide from amyloid-rich pancreases of type 2 diabetic patients, Proc. Natl. Acad. Sci. U. S. A. 84 (1987) 8628–8632.
[3] P. Westermark, C. Wernstedt, E. Wilander, K. Sletten, A novel peptide in the calcitonin gene related peptide family as an amyloid fibril protein in the endocrine pancreas, Biochem. Biophys. Res. Commun. 140 (1986) 827–831.
[4] B. Gedulin, G.J. Cooper, A.A. Young, Amylin secretion from the perfused pancreas: dissociation from insulin and abnormal elevation in insulin-resistant diabetic rats, Biochem. Biophys. Res. Commun. 180 (1991) 782–789.
[5] R.L. Hull, G.T. Westermark, P. Westermark, S.E. Kahn, Islet amyloid: a critical entity in the pathogenesis of type 2 diabetes, J. Clin. Endocrinol. Metab. 89 (2004) 3629–3643.
[6] L. Caillon, A.R.F. Hoffmann, A. Botz, L. Khemtemourian, Molecular structure, membrane interactions and toxicity of the islet amyloid polypeptide in type 2 diabetes mellitus, J. Diabetes Res. (2016) 5639875.
[7] P. Westermark, U. Engstrom, K.H. Johnson, G.T. Westermark, C. Betsholtz, Islet amyloid polypeptide - pinpointing amino-acid-residues linked to amyloid fibril formation, Proc. Natl. Acad. Sci. U. S. A. 87 (1990) 5036–5040.
[8] A. Abedini, D.P. Raleigh, Destabilization of human IAPP amyloid fibrils by proline mutations outside of the putative amyloidogenic domain: is there a critical amyloidogenic domain in human IAPP? J. Mol. Biol. 355 (2006) 274–281.
[9] S. Maurer-Stroh, M. Debulpaep, N. Kuemmerer, M. Lopez de la Paz, I.C. Martins, J. Reumers, K.L. Morris, A. Copland, L. Serpell, L. Serrano, J.W. Schymkowitz, F. Rousseau, Exploring the sequence determinants of amyloid structure using position-specific scoring matrices, Nat. Methods 7 (2010) 237–242.
[10] D.F. Moriaarty, D.P. Raleigh, Effects of sequential proline substitutions on amyloid formation by human amylin20-29, Biochemistry 38 (1999) 1811–1818.
[11] C. Nerelius, M. Fitzen, J. Johansson, Amino acid sequence determinants and molecular chaperones in amyloid fibril formation, Biochem. Biophys. Res. Commun. 396 (2010) 2–6.
[12] L. Tjernberg, W. Hosia, N. Bark, J. Thyberg, J. Johansson, Charge attraction and beta propensity are necessary for amyloid fibril formation from tetrapeptides, J. Biol. Chem. 277 (2002) 43243–43246.
[13] H. Wang, A. Abedini, B. Ruzsicska, D.P. Raleigh, Rationally designed, nontoxic, nonamyloidogenic analogues of human islet amyloid polypeptide with improved solubility, Biochemistry 53 (2014) 5876–5884.
[14] L.H. Tu, D.P. Raleigh, Role of aromatic interactions in amyloid formation by islet amyloid polypeptide, Biochemistry 52 (2013) 333–342.
[15] A. Fox, T. Snollaerts, C. Errecart Casanova, A. Calciano, L.A. Nogaj, D.A. Moffet, Selection for nonamyloidogenic mutants of islet amyloid polypeptide (IAPP) identifies an extended region for amyloidogenicity, Biochemistry 49 (2010) 7783–7789.
[16] A. Abedini, D.P. Raleigh, The role of His-18 in amyloid formation by human islet amyloid polypeptide, Biochemistry 44 (2005) 16284–16291.
[17] J.R. Brender, K. Hartman, K.R. Reid, R.T. Kennedy, A. Ramamoorthy, A single mutation in the nonamyloidogenic region of islet amyloid polypeptide greatly reduces toxicity, Biochemistry 47 (2008) 12680–12688.
[18] L. Khemtémourian, E. Doménech, J.P. Doux, M.C. Koorengevel, J.A. Killian, Low pH acts as inhibitor of membrane damage induced by human islet amyloid polypeptide, J. Am. Chem. Soc. 133 (2011) 15598–15604.
[19] J. Green, C. Goldsbury, T. Mini, S. Sunderji, P. Frey, J. Kistler, G. Cooper, U. Aebi1, Full-length rat amylin forms fibrils following substitution of single residues from human amylin, J. Mol. Biol. 326 (2003) 1147–1156.
[20] P. Marek, A.M. Woys, K. Sutton, M.T. Zanni, D.P. Raleigh, Efficient microwave-assisted synthesis of human islet amyloid polypeptide designed to facilitate the specific incorporation of labeled amino acids, Org. Lett. 12 (2010) 4848–4851.
[21] L. Khemtémourian, G. Lahoz Casarramona, D.P. Suylen, T.M. Hackeng, J.D. Meeldijk, B. de Kruijff, J.A. Killian, Impaired processing of human pro-islet amyloid polypeptide is not a causative factor for fibril formation or membrane damage in vitro, Biochemistry 48 (2009) 10918–10925.
[22] P.J. Marek, V. Patsalo, D.F. Green, D.P. Raleigh, Ionic strength effects on amyloid formation by amylin are a complicated interplay among Debye screening, ion selectivity, and Hofmeister effects, Biochemistry 51 (2012) 8478–8490.
[23] L.M. Green, J.L. Reade, C.F. Ware, Rapid colorimetric assay for cell viability: application to the quantitation of cytotoxic and growth inhibitory lymphokines, J. Immunol. Methods 70 (1984) 257–268.
[24] A.A. Zamyatnin, Protein volume in solution, Prog. Biophys. Mol. Biol. 24 (1972) 107–123.
[25] J. Kyte, R.F. Doolittle, A simple method for displaying the hydropathic character of a protein, J. Mol. Biol. 157 (1982) 105–132.
[26] H. LeVine 3rd, Quantification of beta-sheet amyloid fibril structures with thioflavin T, Methods Enzymol. 309 (1999) 274–284.
[27] L. Caillon, O. Lequin, L. Khemtémourian, Evaluation of membrane models and their composition for islet amyloid polypeptide-membrane aggregation, Biochim. Biophys. Acta 1828 (2013) 2091–2098.
[28] P. Cao, F. Meng, A. Abedini, D.P. Raleigh, The ability of rodent islet amyloid polypeptide to inhibit amyloid formation by human islet amyloid polypeptide has important implications for the mechanism of amyloid formation and the design of inhibitors, Biochemistry 49 (2010) 872–881.
[29] S. Jha, J.M. Snell, S.R. Sheftic, S.M. Patil, S.B. Daniels, F.W. Kolling, A.T. Alexandrescu, pH dependence of amylin fibrillization, Biochemistry 53 (2014) 300–310.
[30] M.J. Thompson, S.A. Sievers, J. Karanicolas, M.I. Ivanova, D. Baker, D. Eisenberg, The 3D profile method for identifying fibril-forming segments of proteins, Proc. Natl. Acad. Sci. U. S. A. 103 (2006) 4074–4078.
[31] A.P. Pawar, K.F. Dubay, J. Zurdo, F. Chiti, M. Vendruscolo, C.M. Dobson, Prediction of “aggregation-prone” and “aggregation-susceptible” regions in proteins associated with neurodegenerative diseases, J. Mol. Biol. 350 (2005) 379–392.
[32] N. Sánchez de Groot, I. Pallarés, F.X. Avilés, J. Vendrell, S. Ventura, Prediction of “hot spots” of aggregation in disease-linked polypeptides, BMC Struct. Biol. 30 (2005) 18.
[33] M. Sebastiao, N. Quittot, S. Bourgault, Thioflavin T fluorescence to analyse amyloid formation kinetics: measurement frequency as a factor explaining irreproducibility, Anal. Biochem. 532 (2017) 83–86.
[34] L.H. Tu, L.M. Young, A.G. Wong, A.E. Ashcroft, S.E. Radford, D.P. Raleigh, Mutational analysis of the ability of resveratrol to inhibit amyloid formation by islet amyloid polypeptide: critical evaluation of the importance of aromatic-inhibitor and histidine-inhibitor interactions, Biochemistry 54 (2015) 666–676.
[35] P. Cao, L.H. Tu, A. Abedini, O. Levsh, R. Akter, V. Patsalo, A.M. Schmidt, D.P. Raleigh, Sensitivity of amyloid formation by human islet amyloid polypeptide to mutations at residue 20, J. Mol. Biol. 421 (2012) 282–295.
[36] D.T. Meier, L. Entrup, A.T. Templin, M.F. Hogan, M. Mellati, S. Zraika, R.L. Hull, S.E. Kahn, The S20G substitution in hIAPP is more amyloidogenic and cytotoxic than wild-type hIAPP in mouse islets, Diabetologia 59 (2016) 2166–2171.
[37] W. Xu, P. Jiang, Y. Mu, Conformation preorganization: effects of S20G mutation on the structure of human islet amyloid polypeptide segment, J. Phys. Chem. B 113 (2009) 7308–7314.
[38] N.N. Louros, P.L. Tsiolaki, A.A. Zompra, E.V. Pappa, V. Magafa, G. Pairas, P. Cordopatis, C. Cheimonidou, I.P. Trougakos, V.A. Iconomidou, S.J. Hamodrakas, Structural studies and cytotoxicity assays of “aggregation-prone” IAPP(8-16) and its non-amyloidogenic variants suggest its important

role in fibrillogenesis and cytotoxicity of human amylin, Biopolymers 104 (2015) 196–205.
[39] B.W. Koo, J.A. Hebda, A.D. Miranker, Amide inequivalence in the fibrillar assembly of islet amyloid polypeptide, Protein Eng. Des. Sel. 21 (2008) 147–154.
[40] L.H. Tu, A.L. Serrano, M.T. Zanni, D.P. Raleigh, Mutational Analysis of Pre-amyloid Intermediates: the role of His-Tyr interactions in islet amyloid formation, Biophys. J. 106 (2014) 1520–1527.
[41] S. Luca, W.M. Yau, R. Leapman, R. Tycko, Peptide conformation and supramolecular organization in amylin fibrils: constraints from solid-state NMR, Biochemistry 46 (2007) 13505–13522.
[42] S. Bedrood, Y. Li, J.M. Isas, B.G. Hegde, U. Baxa, I.S. Haworth, R. Langen, Fibril structure of human islet amyloid polypeptide, J. Biol. Chem. 287 (2012) 5235–5241.
[43] J.R. Brender, K. Hartman, R.P.R. Nanga, N. Popovych, R. de la Salud Bea, S. Vivekanandan, E.N. Marsh, A. Ramamoorthy, Role of zinc in human islet amyloid polypeptide aggregation, J. Am. Chem. Soc. 132 (2010) 8973–8983.
[44] S.J.C. Lee, T.S. Choi, J.W. Lee, H.J. Lee, D.-G. Mun, S. Akashi, Structure and assembly mechanisms of toxic human islet amyloid polypeptide oligomers associated with copper, Chem. Sci. 7 (2016) 5398–5406.
[45] S. Salamekh, J.R. Brender, S.-J. Hyung, R.P.R. Nanga, S. Vivekanandan, B.T. Ruotolo, A. Ramamoorthy, A two-site mechanism for the inhibition of IAPP amyloidogenesis by zinc, J. Mol. Biol. 410 (2011) 294–306.
[46] D.S. Yang, J. McLaurin, K. Qin, D. Westaway, P.E. Fraser, Examining the zinc binding site of the amyloid-beta peptide, Eur. J. Biochem. 267 (2000) 6692–6698.
[47] A.N. Istrate, S.A. Kozin, S.S. Zhokhov, A.B. Mantsyzov, O.I. Kechko, A. Pastore, A.A. Makarov, V.I. Polshakov, Interplay of histidine residues of the Alzheimer's disease Aβ peptide governs its Zn-induced oligomerization, Sci. Rep. 6 (2016) 21734.
[48] A.S. DeToma, S. Salamekh, A. Ramamoorthy, M.H. Lim, Misfolded proteins in Alzheimer's disease and type II diabetes, Chem. Soc. Rev. 41 (2012) 608–621.
[49] D.P. Smith, D.G. Smith, C.C. Curtain, J.F. Boas, J.R. Pilbrow, G.D. Ciccotosto, T.L. Lau, D.J. Tew, K. Perez, J.D. Wade, A.I. Bush, S.C. Drew, F. Separovic, C.L. Masters, R. Cappai, K.J. Barnham, Copper-mediated amyloid-beta toxicity is associated with an intermolecular histidine bridge, J. Biol. Chem. 281 (2006) 15145–15154.
[50] Y. Porat, A. Abramowitz, E. Gazit, Inhibition of amyloid fibril formation by polyphenols: structural similarity and aromatic interactions as a common inhibition mechanism, Chem. Biol. Drug. Des. 67 (2006) 27–37.
[51] Y. Porat, Y. Mazor, S. Efrat, E. Gazit, Inhibition of islet amyloid polypeptide fibril formation: a potential role for heteroaromatic interactions, Biochemistry 43 (2004) 14454–14462.
[52] A. Abedini, F. Meng, D.P. Raleigh, A single-point mutation converts the highly amyloidogenic human islet amyloid polypeptide into a potent fibrillization inhibitor, J. Am. Chem. Soc. 129 (2007) 11300–11301.
[53] L.M. Yan, A. Velkova, M. Tatarek-Nossol, E. Andreetto, A. Kapurniotu, IAPP mimic blocks Abeta cytotoxic self-assembly: cross-suppression of amyloid toxicity of Abeta and IAPP suggests a molecular link between Alzheimer's disease and type II diabetes, Angew. Chem. Int. Ed. Engl. 46 (2007) 1246–1252.
[54] L.M. Yan, A. Velkova, M. Tatarek-Nossol, G. Rammes, A. Sibaev, E. Andreetto, M. Kracklauer, M. Bakou, E. Malideli, B. Göke, J. Schirra, M. Storr, A. Kapurniotu, Selectively N-methylated soluble IAPP mimics as potent IAPP receptor agonists and nanomolar inhibitors of cytotoxic self-assembly of both IAPP and Aβ40, Angew. Chem. Int. Ed. Engl. 52 (2013) 10378–10383.